Kinetics of Manganese Chloride in Non-CNS Organs in Mice

L-W. Lee[1], P-W. So[2], A. Price[1], J. Halliday[3], S. M. Poucher[3], J. A. Pugh[4], C. W. McLeod[4], and J. D. Bell[1]

[1]Metabolic and Molecular Imaging Group, Imaging Sciences Department, MRC Clinical Sciences Centre, Hammersmith Hospital Campus, Imperial College London, London, United Kingdom, [2]Biological Imaging Centre, Imaging Sciences Department, MRC Clinical Sciences Centre, Hammersmith Hospital Campus, Imperial College London, London, United Kingdom, [3]AstraZeneca Pharmaceuticals, Macclesfield, United Kingdom, [4]Centre for Analytical Sciences, University of Sheffield, Sheffield, United Kingdom

Introduction

Ca^{2+} signals play a major role both in normal cellular functions and pathological processes including exocytosis, contraction, metabolism, transcription, fertilization and proliferation[1] in most cell types. Similar to Ca^{2+}, Mn^{2+} is taken up by cells via Ca^{2+} transport pathways where its paramagnetic properties afford signal enhancement in T_1-weighted MRI methodologies. Therefore, manganese-enhanced MRI (MEMRI) is a novel imaging technique capable of monitoring Ca^{2+} influx. Currently, MEMRI has been used to image cellular activity in the brain and heart and may have the potential to image other cell types in which Ca^{2+} plays a role in cellular signaling, such as in platelets[2,3], lymphocytes[4], endothelial cells[5], neurtrophils[6], parotid acinar cells[7], adrenal chromaffin cells[8] and mast cells[9]. Here, we implement both *in vivo* MRI as well as *in vitro* quantification of absolute tissue manganese (Mn) content to determine distribution of Mn^{2+} following i.v. infusion. In addition, we use a magnetization-prepared rapid gradient echo (MP-RAGE) sequence based MEMRI to demonstrate a significantly increased signal enhancement in the murine pancreas following stimulation by peripheral glucose administration.

Materials and Methods

All MRI studies were performed on a 4.7T MRI scanner. Mice were imaged under terminal inhalation anesthesia. T_1 measurements were performed on $MnCl_2$ solutions (0-1mM), using inversion recovery spin-echo (IR-SE) and MP-RAGE with TI = 20-4500ms. For *in vivo* T1 measurements C57BL/6 mice were fasted overnight prior to MRI. MP-RAGE was acquired 6min after tail vein infusion of $MnCl_2$ (2 - 40mM 0.1ml, 0.2ml/h); acquisition time was 30min. After MRI, tissues were collected and kept at -80°C prior to assessment of tissue Mn content by induction-coupled-plasma emission spectrometry (ICP-ES). For time-course studies, MP-RAGE (TI = 740ms, TD = 2s) was acquired prior to and following $MnCl_2$ infusion (2mM, 0.1ml, 0.2ml/h). For glucose challenge (or vehicle, control), a bolus i.p. injection of 2g/kg glucose was administered at 16min after start of $MnCl_2$ infusion. In a model of diabetes, mice were injected i.p. with 170-180mg/kg streptozotocin (STZ) and MEMRI performed in mice when fed blood glucose >20mmol/L. Pancreata from Mn^{2+} treated and non-treated mice were also collected for histological analysis to determine any pathological effects of the Mn^{2+} dose. All data were presented as mean ± sem.

Results and Conclusions

T_1 and R_1 values of $MnCl_2$ solutions as measured by IR-SE and MP-RAGE are shown in Figure 1. There is a good agreement between the two measuring methods at low [Mn^{2+}]. However, an overestimation of R_1 values was seen at higher [Mn^{2+}] in the MP-RAGE data. Subsequent *in vivo* R_1 values obtained by MP-RAGE were therefore normalized to the standard curve in Figure 1. Figure 2 shows the relationship between R_1 values and tissue Mn content (as measured by ICP-ES), following increasing systemic doses of $MnCl_2$. There was a strong linear correlation between R_1 values and tissue Mn content in the pancreas ($r^2 = 0.9394$), kidney ($r^2 = 0.9179$), liver ($r^2 = 0.9834$) and heart ($r^2 = 0.9529$) (Figure 2). Tissue Mn was low in the muscle, spleen and fat, and reflected in the R1 values measured (Figure 2). At the lowest dose of $MnCl_2$ (2mM, 0.1ml), pancreatic islets were shown to be unaffected (hematoxylin and eosin staining, data not shown). Figure 3 shows the affect of an i.p. dose of glucose (and water, control) on the MEMRI signal intensity (SI) profiles in the mouse pancreas of both non-STZ-treated and STZ-treated mice. The SI in the pancreatic ROI rises following $MnCl_2$ administration reaching peak enhancement soon after the end of infusion in all 4 groups. However, there was significantly greater signal enhancement in the mouse pancreas of up to 45% in glucose-stimulated non-STZ-treated group compared with the other three groups ($p<0.05$, GEE) (Figure 3).

In conclusion, we have shown that MP-RAGE based MRI is an effective means of monitoring Mn^{2+} *in vivo* in non-brain organs, following i.v. infusion, with the estimated T_1 values aiding determination of the optimal MRI parameters at 4.7T. The dose-dependent Mn^{2+} distribution in major non-brain organs as assessed by this methodology provides a practical $MnCl_2$ dosing regimen for use in tissue-specific activation studies. Further, we demonstrate that MP-RAGE can be used to record significantly increased signal enhancements in the murine pancreas following glucose stimulation. This study provides a potential 3D-MRI technique for *in vivo* imaging of Ca^{2+} entry during Ca^{2+}-dependent processes in a wide range of tissues.

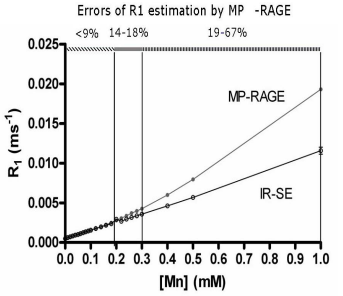

Figure 1. Comparison of R_1 values measured by IR-SE and MP-RAGE *in vitro* of various [$MnCl_2$], (n=3/group).

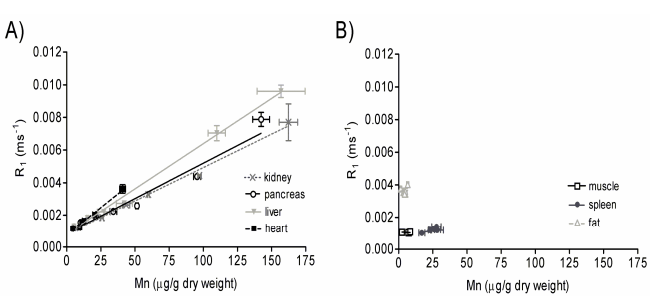

Figure 2. Tissue-specific relationships between R_1 values and Mn content. R_1 values and tissue manganese (n=3/group), as measured by MRI and ICP-ES, respectively, shows a linear relationship.

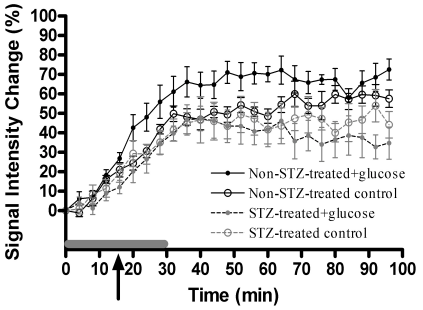

Figure 3. Pancreatic SI profiles after peripheral administration of glucose in non-STZ-(control) treated (n=6/group) and STZ-treated (diabetic) mice (n=4/group). The grey bar indicates the start and duration of the i.v. $MnCl_2$ infusion. The arrow indicates the bolus i.p. injection of glucose or distilled water (control).

References

1.*Nat Rev Mol Cell Biol* 4, 517-29 (2003). 2.*Annu Rev Physiol* 52, 431-49 (1990). 3.*FEBS Lett* 186, 175-9 (1985). 4.*Am J Physiol* 265, C321-7 (1993). 5.*Biochem J* 255, 179-84 (1988). 6.*J Biol Chem* 264, 1522-7 (1989). 7.*J Biol Chem* 265, 15010-4 (1990). 8.*Cell Calcium* 19, 419-29 (1996). 9.*Proc Natl Acad Sci U S A* 90, 3068-72 (1993).